Synergistic Effect of Halide Ions on the Corrosion Inhibition of Mild Steel in Hydrochloric Acid using Mangrove Tannin

A.M. Ridhwan , A.A. Rahim[*]*, A.M. Shah*

School of Chemical Sciences, Universiti Sains Malaysia, 11800 Pulau Pinang, Malaysia
[*]E-mail: afidah@usm.my

The inhibitive effect of mangrove tannin (MT) on mild steel (MS) corrosion in 0.5 M hydrochloric acid solution was studied using electrochemical techniques and gravimetric method. The influence of halides viz., KCl, KBr and KI on the corrosion inhibition of MT were also investigated. Results show that MT alone provided satisfactory inhibition on the corrosion of MS and it was also found that the inhibition efficiency increased synergistically in the presence of halide ions. The synergistic effect of halide ions was found to follow the order: KI > KBr > KCl. The inhibitor reduced the corrosion rate through adsorption process and obeyed the Langmuir's adsorption isotherm.

1. INTRODUCTION

The corrosion behaviour of mild steel has been widely investigated in several environments. Corrosion of metals such as mild steel is an electrochemical reaction which can cause the degradation and damage of the physical and chemical properties of the attacked metal. Besides the natural factors such as air humidity and wetness time, the usage of acid is found to be the major factor that drives to the corrosion problem. Strong acids like hydrochloric acid and sulphuric acid are widely used in industries for many purposes especially for pickling, cleaning, de-scaling, etc. In order to reduce the undesirable acid metal dissolution, the use of inhibitors is one of the most practical methods for the surface protection against the corrosive media especially in acidic environments. The effectiveness of the inhibition normally relies on the type of the metal studied and the concentration of the inhibitor itself [1].

Owing to the concern in environmental matters and the need to develop environmentally friendly processes, attention is now focused on the development of nontoxic alternatives to replace the inorganic inhibitors which are harmful to the environment. Recently, natural products extracted from plant sources have become important as an environmentally acceptable, readily available and renewable source for a wide range of corrosion inhibitors. Several investigations have been reported to use plant extracts as inhibitors that contained alkaloids, polyphenolic compounds as well as carbohydrates [2-3]. Furthermore, most of the organic active inhibitors components consisted of at least a polar group with an atom of nitrogen, sulphur or oxygen [4-8]. It has been reported that most of the effective inhibitors possess an active functional group such as nitro ($-NO_2$) or a hydroxyl (-OH) group [9]. Tannin which is extracted from the mangrove bark is a phenolic compound with high molecular mass and consists of hydroxyl groups. Tannin was found to be a good corrosion inhibitor for mild steel in acidic media [10].

Most acid inhibitors are known for their specificity of action. However, the addition of other substances and the combination of inhibitors has provided multiple effects of effective corrosion inhibition. Interestingly, the addition of halide ions into the acidic medium in the presence of organic inhibitors has been found to enhance the efficiency of inhibitive effects [11-14]. It is generally seen that the addition of halide ions to the corrosive media has increased the ability of adsorption of the organic cations by forming the interconnecting bridge between negatively charge metal surface and inhibitor cations. The introduction of the halide ions synergistically enhanced the inhibition efficiency of the organic inhibitors [15-22].

In this present work, we have studied the inhibition effect of mangrove tannin (MT) on the corrosion of mild steel in 0.5 M HCl solution. Then, we attempted to enhance the inhibition efficiency further by the addition of halide ions namely iodide (I^-), bromide (Br^-) and chloride (Cl^-) to the MT.

2. EXPERIMENTAL

2.1. Material preparation

Tests were performed on mild steel sheets with weight percentage composition as follows: C, 0.205; Mn, 0.55; Si, 0.06; P, 0.039; Fe, balance. The sheets (0.1 cm thickness) were mechanically cut into dimensions of 3.0 cm x 1.0 cm for weight loss studies and 3.0 cm x 3.0 cm for electrochemical studies. The studied surface was wet-polished with silicon carbide abrasive paper (from grade 400 to 1200), rinsed with double distilled water and degreased in acetone and dried in warm air.

2.2. Inhibitor preparation

The finely ground mangrove bark powder was mixed with 70% acetone and stirred for 24 hours. This extract solution was then concentrated at 40 ℃ under reduced pressure in a rotary evaporator to remove the acetone. Then, the concentrated extract was frozen for 24 hours before being

freeze-dried for 48 hours. The test inhibitor MT obtained was dissolved in 0.5 M HCl solution to obtain the desired concentration (3.0 g L^{-1}). Potassium iodide (KI), potassium bromide (KBr) and potassium chloride (KCl) solutions ($1 \times 10^{-5} - 1 \times 10^{-1}$ M) were prepared in the blank solution and in 3.0 g L^{-1} MT, respectively.

2.3. Weight loss measurements

In the weight loss measurements, the pre-cleaned mild steel coupons were suspended in 100 mL of test solutions maintained at room temperature (27±2 ºC). All tests were made in aerated solutions. The weight loss was determined after immersing the coupons for 7 days, rinsed in distilled water, degreased in acetone, dried and reweighed. The weight loss was taken to be the difference between the weight of coupons at a given time and its initial weight. The percentage inhibition efficiency (IE) was calculated by Eq. (1).

$$IE = \frac{W_{\circ} - W_i}{W_{\circ}} \times 100 \qquad (1)$$

Where $W_{\circ}$ is the weight loss of mild steel in the absence of inhibitor and W_i is the weight loss of mild steel in the presence of inhibitor.

2.4. Electrochemical studies

Electrochemical measurements were conducted in a conventional three-electrode cell of capacity 50 mL. Mild steel coupons were used as a working electrode while a saturated calomel electrode (SCE) and a platinum electrode were used as reference and counter electrode, respectively. The potentiodynamic polarisation analysis was carried out using Potentiostat/Galvanostat/ZRA Model Gamry Reference 600 and the data were analysed using Gamry Instrument Framework version 5.57 software. The electrode was held in the test solution at the natural potential for 30 minutes which provided sufficient time for E_{corr} to attain a reliable stable state in the open circuit potential (E_{ocp}). Electrochemical impedance spectroscopy (EIS) measurements were made at corrosion potential (E_{corr}) over the frequency range from 100,000 to 0.1 Hz at an amplitude of 10 mV and scan rate of 10 points per decade. The Nyquist representations of the impedance data were analysed with ZSimpWin software. The charge transfer resistance (R_{ct}) was obtained from the diameter of the semicircle in Nyquist representation. The inhibition efficiency (IE) of the inhibitor is calculated from the relationship,

$$IE = \frac{R'_{ct} - R_{ct}}{R'_{ct}} \times 100 \qquad (2)$$

Where R_{ct} and R'_{ct} are the charge transfer resistance values in the absence and presence of inhibitors, respectively.

The polarisation measurement was carried out from a cathodic potential of -0.2 V to an anodic potential of +0.2 V with respect to the E_{corr} at a sweep rate of 1 mVs^{-1}. The linear Tafel segments of anodic and cathodic curves (-0.2 to +0.2 V vs E$_{ocp}$) were extrapolated to E_{corr} to obtain the corrosion current density (i_{corr}). The inhibition efficiency (IE) was obtained from the measured i_{corr} using the following relationship:

$$IE = \frac{i_o - i}{i_o} \times 100 \qquad (3)$$

Where i and i_o are the inhibited and uninhibited corrosion current densities, respectively.

3. RESULTS AND DISCUSSION

3.1. Weight loss measurements

Table 1. Inhibition efficiency values for mild steel in 0.5 M HCl solution in the absence and presence of MT and KI from weight loss measurement at 27±2 ºC for 7 days of immersion time.

System/concentration	Weight loss (g)	%IE
Blank	0.2597	-
3 g L^{-1} MT	0.0404	84.44
1 × 10^{-5} M KI	0.1859	28.42
3 g L^{-1} MT + 1 × 10^{-5} M KI	0.0402	84.52
1 × 10^{-4} M KI	0.1708	34.23
3 g L^{-1} MT + 1 × 10^{-4} M KI	0.0138	94.69
1 × 10^{-3} M KI	0.1182	54.49
3 g L^{-1} MT + 1 × 10^{-3} M KI	0.0100	96.15
1 × 10^{-2} M KI	0.0652	74.89
3 g L^{-1} MT + 1 × 10^{-2} M KI	0.0093	96.42
1 × 10^{-1} M KI	0.0432	83.37
3 g L^{-1} MT + 1 × 10^{-1} M KI	0.0061	97.65

The corrosion of mild steel in 0.5 M HCl in the absence and presence of MT as inhibitor, halides and combination of halides with MT was studied using the weight loss technique at room temperature (27±2 ºC). The inhibition efficiency as a function of concentration of inhibitors is shown in Table 1. It is observed that as the MT was introduced to the corrodent solution, the weight loss of the mild steel was reduced while the inhibition efficiency increased (up to 84.44%). It can also be seen from Table 1 that after the addition of KI into the HCl solution with MT, corrosion rates decreased significantly in comparison with MT alone. As shown in Table 1, when 1 × 10^{-1} M KI was added into the 0.5 M HCl solution containing 3 g L^{-1} MT, the weight loss reduced from 0.0404 to 0.0061 g. Accordingly, the percentage of inhibition efficiency increased up to 97.65%. These results suggest that

there is a synergistic effect between inhibitor molecules and halide ions. In addition, it has been found that different halide ions resulted in different extent of inhibition efficiency (not shown). The order of synergism of halide ions was found to be in the order of KI > KBr > KCl with percentage of inhibition efficiency given by the highest concentration of each halide ions (1×10^{-1} M) where KCl (up to 95.15% – not shown), followed by KBr (up to 95.92% – not shown) and KI which acquiesce to 97.65% efficiency. Clearly, the iodide has the strongest synergistic effect among the three halides and thus will be focused.

3.2. Polarisation measurements

The potentiodynamic polarisation behaviour of mild steel in 0.5 M HCl with and without different concentrations of KI is shown in Figure 1 and Figure 2, respectively. It is clear from the figures that the addition of MT has slightly shifted the E_{corr} to negative values and reduced both the anodic iron dissolution and cathodic hydrogen evolution reactions. However, in the presence of MT and halide ions, the curves shifted more toward positive potential values. Corrosion current densities reduced markedly in the presence of MT compared to its absence. The related electrochemical parameters such as i_{corr}, E_{corr}, the cathodic Tafel slope (β_c) and anodic Tafel slope (β_a) obtained from the polarisation curves are listed in Table 2. The results in the tables indicated that i_{corr} decreased significantly when MT was combined with the halide ions.

The E_{corr} values were shifted slightly positive in the combination of MT with both KCl and KBr while significantly shifted positively when combined with the KI. This indicates that the anodic reaction was drastically inhibited [23] in the presence of both MT and KI. Both KCl and KBr showed the same trend of Tafel behaviour, while KI showed some differences. As shown in both Figure 1 and Figure 2, the Tafel plot in the presence of KI showed higher gradients on the anodic side as compared to the cathodic region. This is due to the phenomenon of mass transport whereby there is a formation of dissolved metal ions at the corroding surface. Consequently, these ions will diffuse towards the bulk solution and resulted in the existence of a concentration gradient in the diffusion layer adjacent to the electrode [24].

The inhibition efficiencies for MT alone and in combination with KI were calculated and also listed in the tables. The addition of halide ions has slightly improved the value of inhibition efficiency of MT (from 63.91% up to 85.38% in KCl – not shown, 91.85% in KBr – not shown and 93.66% in KI). Although the anodic and cathodic currents were significantly reduced when both MT and halide ions were present, a low polarisation current was observed, indicating a synergistic effect has occurred between MT and halide ions [25]. On the other hand, the anodic and cathodic Tafel slopes changed irregularly with the addition of MT alone and in combination with the halide ions. The changes in Tafel slope in the presence of inhibitors indicate that the corrosion mechanism is changed. The increasing of halide ions concentrations slightly improved the value of inhibition efficiency of MT. All parameters obtained from the polarisation measurements were found to be concentration dependent of the halide ions.

Table 2. Potentiodynamic polarisation parameters for mild steel in 0.5 M HCl solution in the absence and presence of MT and KI.

System/concentration	-βa (mV dec-1)	-βc (mV dec-1)	Ecorr (mV)	Icorr (μA cm-2)	IE
Blank	65.90	101.60	- 491.0	77.30	-
3 g L^{-1} MT	73.40	155.80	- 457.0	27.90	63.91
1×10^{-5} M KI	94.90	100.50	- 497.0	84.20	- 8.93
3 g L^{-1} MT + 1×10^{-5} M KI	55.10	157.70	- 427.0	12.30	84.09
1×10^{-4} M KI	92.20	94.30	- 495.0	55.80	27.81
3 g L^{-1} MT + 1×10^{-4} M KI	50.10	156.60	- 420.0	10.60	86.29
1×10^{-3} M KI	81.60	122.50	- 466.0	44.30	42.69
3 g L^{-1} MT + 1×10^{-3} M KI	44.10	149.70	- 410.0	6.90	91.07
1×10^{-2} M KI	42.40	68.50	- 432.0	9.98	87.09
3 g L^{-1} MT + 1×10^{-2} M KI	32.10	96.30	- 393.0	4.90	93.66
1×10^{-1} M KI	46.10	107.90	- 382.0	39.00	49.55
3 g L^{-1} MT + 1×10^{-1} M KI	16.40	121.20	- 330.0	12.30	84.09
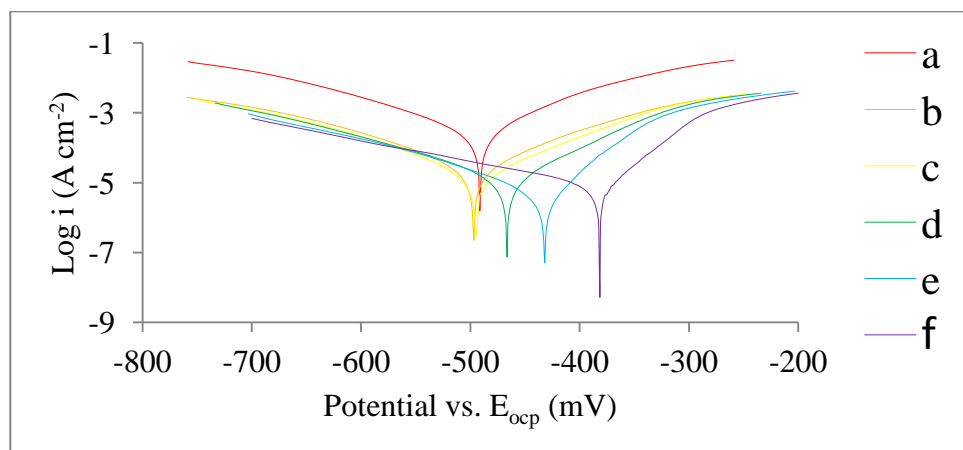
Figure 1. Polarisation curves of mild steel immersed in 0.5 M HCl at different concentration of KI: (a) blank; (b) 1×10^{-5} M; (c) 1×10^{-4} M; (d) 1×10^{-3} M; (e) 1×10^{-2} M; (f) 1×10^{-1} M
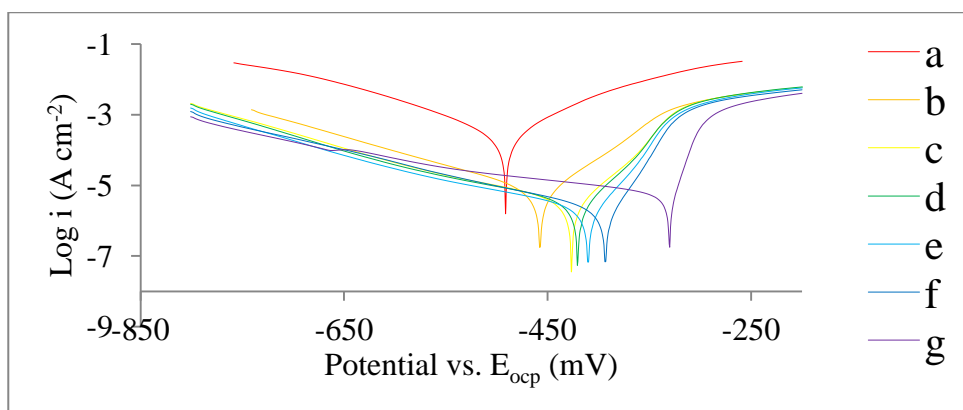
Figure 2. Polarisation curves of mild steel in 0.5 M HCl in the presence of MT at different concentration of KI: (a) blank; (b) 3 g L^{-1} MT; (c) 3 g L^{-1} MT + 1×10^{-5} M; (d) 3 g L^{-1} MT + 1×10^{-4} M; (e) 3 g L^{-1} MT + 1×10^{-3} M; (f) 3 g L^{-1} MT + 1×10^{-2} M; (g) 3 g L^{-1} MT + 1×10^{-1} M

3.3. Electrochemical impedance spectroscopy (EIS)

The measurements were undertaken to assess the interactions of the mild steel/electrolyte interface in the presence and absence of MT with different concentrations of halide ions. The impedance data for mild steel in 0.5 M HCl with and without MT and in combination with KI were recorded and listed in Table 3. The Nyquist plots for mild steel in the presence and absence of MT and in the combination with KI are shown in Figure 3 and Figure 4, respectively. It is observed that increasing the concentration of KI with and without the combination with MT results in an increase in the size of the semicircle, indicating inhibition of corrosion process. All Nyquist plots at high frequencies obtained in all processes are not perfect semicircle but depressed. The depressed form of semicircles is often referred to as frequency dispersion which has been attributed to surface heterogeneity of structural or interfacial origin such as those found in adsorption processes [26]. The surface heterogeneity usually results from surface roughness, impurities or dislocations, fractal structures, distribution of activity centers, adsorption of inhibitors, and formation of porous layers. Similar results have been reported for mild steel in HCl [27-29].

As shown in both Figure 3 and Figure 4, the impedance response of mild steel in HCl solution with different concentrations of KI and in the presence and absence of MT is characterized by diffusion tail. Hence, the presence of KI at higher concentrations introduces the diffusion step in the corrosion process and the reaction becomes diffusion-controlled. As a result, the corrosion process can occur in two steps as in any electrochemical process at the electrochemical interface. First, the oxidation of the metal (charge transfer process) and followed by the diffusion of the metallic ions from the metal surface to the solution (mass transport process). This case of mass transport supports the results given in the polarisation method. Similar observations were recorded for corrosion inhibition of mild steel in hydrochloric acid solution [30].

The EIS spectra for all tests were analysed by fitting to the equivalent circuit model shown in Figure 5, which represents a single charge transfer reaction. The model has been used previously to model the mild steel/acid interface [26, 31]. The circuit comprises a solution resistance, R_s shorted by a constant phase element (CPE) that is placed in parallel to the charge transfer resistance, R_{ct}. In the evaluation of Nyquist plots, the difference in real impedance at lower and higher frequencies is commonly considered as a charge transfer resistance. The value of charge transfer resistance indicates the electron transfer across the interface. The CPE is used instead of double layer capacitance, C_{dl} in the equivalent circuit in order to fit the data more accurately [32-33]. The introduction of such a CPE is often used to interpret data for the rough solid electrodes. Furthermore, there is a parameter obtained to measure the non-ideality of the capacitor which known as surface irregularity, n which has a value range of $0 < n < 1$. If the electrode surface is homogeneous and plane, the value of n approaching 1 where the metal-solution interface acts as capacitor with regular surface and vice versa [34]. The decrease of n values in the presence of both MT and halides ions could be explained by increment in surface heterogeneity, probably due to the heterogeneous distribution of adsorption of MT and halide ions on the active sides.

From all parameters obtained, it is observed that introduction of MT into the acid solution leads to the increase in the charge transfer resistance and reduction in the constant phase element, which

become more pronounced as the MT is combined with the halide ions. The decrease in CPE values normally results from the decrease in the dielectric constant and/or an increase in the double-layer thickness which leads to a higher inhibition efficiency. In other words, this is due to inhibitor adsorption onto the metal/electrolyte interface [35]. The increase in R_{ct} and the decrease in CPE values as shown in Table 3 are probably due to the replacement of water molecules by halide ions and MT molecules onto the electrode surface, and also may be due to the increase in double layer thickness as a consequence of adsorption of MT and halide ions. As a result, the inhibition efficiency for MT has increased from 85.50 up to 86.10% - not shown (MT + KCl), 78.49% - not shown (MT + KBr) and 97.74% (MT + KI). These values are in good agreement with the potentiodynamic polarisation and weight loss measurements.

Table 3. Electrochemical impedance parameters for mild steel in 0.5 M HCl solution in the absence and presence of MT and KI.

| System/concentration	Rs (Ω cm2)	CPE (μF cm-2)	n	Rct (Ω cm2)	IE
Blank	2.703	223.90	0.9252	57.29	-
3 g L^{-1} MT	2.446	164.50	0.8735	395.20	85.50
1×10^{-5} M KI	2.882	199.60	0.9276	60.16	4.77
3 g L^{-1} MT + 1×10^{-5} M KI	2.395	147.50	0.8807	443.90	87.09
1×10^{-4} M KI	2.821	176.10	0.9188	105.70	45.80
3 g L^{-1} MT + 1×10^{-4} M KI	2.376	126.70	0.8824	515.80	88.89
1×10^{-3} M KI	2.747	169.30	0.9107	168.30	65.96
3 g L^{-1} MT + 1×10^{-3} M KI	2.348	92.31	0.8862	772.20	92.58
1×10^{-2} M KI	2.704	153.60	0.8895	444.20	87.10
3 g L^{-1} MT + 1×10^{-2} M KI	2.295	71.51	0.9059	1356.00	95.78
1×10^{-1} M KI	2.594	130.20	0.8976	778.00	92.64
3 g L^{-1} MT + 1×10^{-1} M KI	2.237	54.40	0.9023	2530.00	97.74
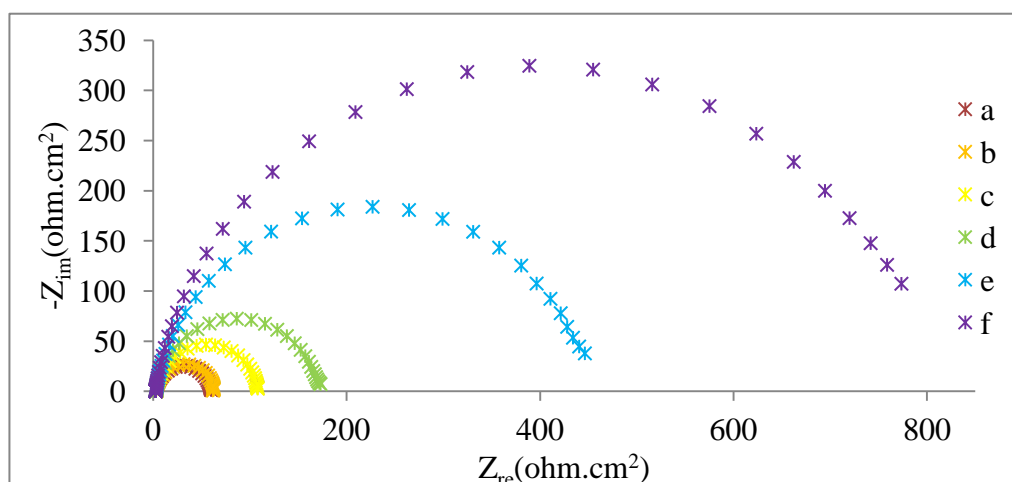
Figure 3. Nyquist plots of mild steel in 0.5 M HCl at different concentration of KI: (a) blank; (b) 1×10^{-5} M; (c) 1×10^{-4} M; (d) 1×10^{-3} M; (e) 1×10^{-2} M; (f) 1×10^{-1} M
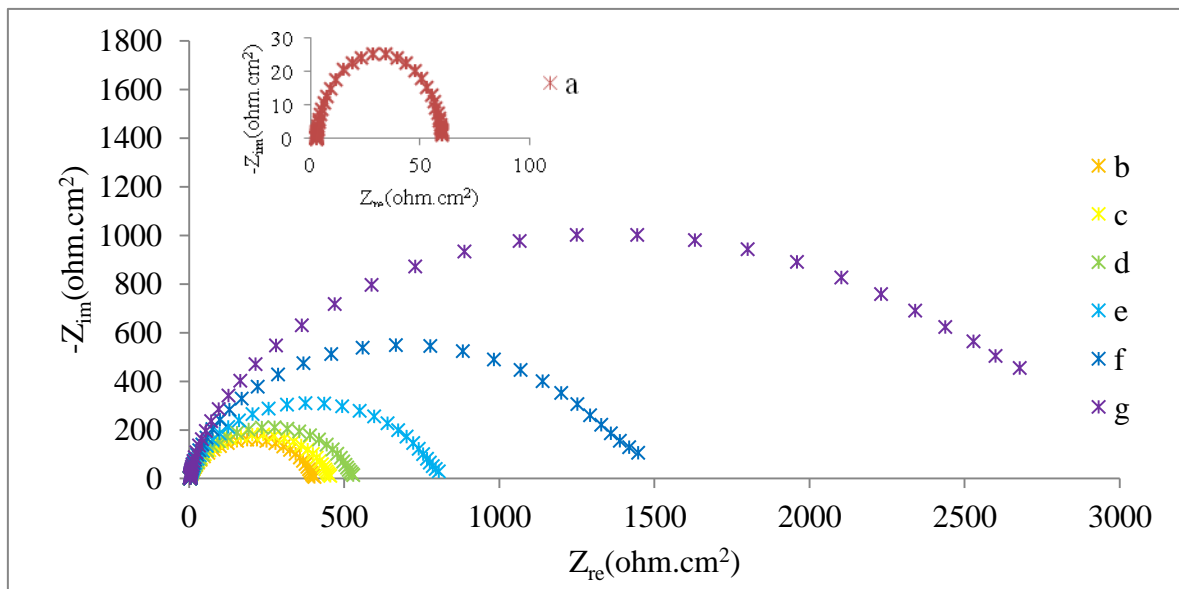
Figure 4. Nyquist plots of mild steel in 0.5 M HCl in the presence of MT at different concentration of KI: (a) blank; (b) 3 g L^{-1} MT; (c) 3 g L^{-1} MT + 1 × 10^{-5} M; (d) 3 g L^{-1} MT + 1 × 10^{-4} M; (e) 3 g L^{-1} MT + 1 × 10^{-3} M; (f) 3 g L^{-1} MT + 1 × 10^{-2} M; (g) 3 g L^{-1} MT + 1 × 10^{-1} M
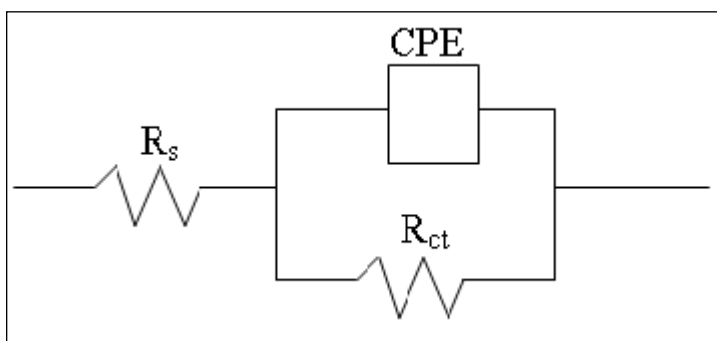
Figure 5. Equivalent circuit model used to fit the impedance data for Nyquist plots

3.4. Adsorption isotherm

Adsorption isotherm calculation of the MT on the mild steel surface in the presence and absence of halide ions were performed to investigate the mode of adsorption. Surface coverage values (θ) (defined as $\theta = \%IE/100$) were evaluated from IE obtained from weight loss, potentiodynamic as well as EIS measurements in order to yield the best fit isotherm model [29]. In order to study the different types of adsorption isotherm models, the Temkin, Freundlich, Frumkin and Langmuir models have been plotted. However, the linear regression (R^2) values of the linear graph obtained (except for Langmuir model) were less than 0.500 (not shown). This indicated that the data does not follow the Temkin, Freundlich or Frumkin adsorption isotherm model. According to the R^2 values obtained from the linear graph, it was confirmed that the adsorption of MT on a mild steel surface best fitted the Langmuir adsorption isotherm model which is represented by Eq. (4).

$$\frac{C_{inh}}{\theta} = \frac{1}{K_{ads}} + C_{inh} \qquad\qquad (4)$$

Where C_{inh} is the concentration of inhibitor and K_{ads} is the adsorption constant, which is related to the standard free energy adsorption, ΔG^{o}_{ads} at a single temperature as follows [36-37]:

$$\Delta G^{\circ}_{ads} = -RT \ln(1000 K_{ads}) \qquad\qquad (5)$$

Where 1000 is the concentration of water in solution expressed in g L^{-1}, R is the molar gas constant and T is the temperature (27±2 °C).

The plots of C_{inh}/θ against C_{inh} for KI for all types of measurement are given in Figure 6 and Figure 7. This plot yields straight lines with linear regression, R^2 values of 0.999 and 1.000. This supports the assumption that the adsorption of MT in the presence and absence of the KI on a mild steel surface in   0.5 M HCl solutions follow the Langmuir adsorption isotherm [38].

Table 4. The parameters of the linear regression from the Langmuir adsorption isotherm for different halide ions.

Method	Inhibitor	Slope	R2	K (L g -1)	ΔG°ads (kJ mol-1)
Potentiodynamic Polarisation	KCl	1.729	0.999	3.45×10^{1}	-26.06
	KCl + MT	1.017	1.000	1.00×10^{3}	-34.46
	KBr	1.119	0.980	2.31×10^{0}	-18.73
	KBr + MT	1.025	1.000	1.00×10^{3}	-34.46
	KI	1.124	0.999	6.17×10^{0}	-21.77
	KI + MT	1.019	1.000	2.50×10^{2}	-31.00
	KCl	2.751	0.999	3.64×10^{-1}	-23.90
Electrochemical Impedance Spectroscopy (EIS)	KCl + MT	1.016	1.000	1.11×10^{5}	-40.46
	KBr	4.516	0.672	9.97×10^{-2}	-11.48
	KBr + MT	1.023	1.000	5.00×10^{2}	-32.73
	KI	0.940	0.945	9.07×10^{-1}	-16.99
	KI + MT	1.002	1.000	1.00×10^{3}	-34.46
	KCl	1.357	1.000	3.13×10^{1}	-25.81
Weight Loss (WL)	KCl + MT	1.050	1.000	1.43×10^{2}	-29.61
	KBr	1.263	0.999	1.39×10^{1}	-23.79
	KBr + MT	1.041	1.000	1.11×10^{2}	-28.98
	KI	1.195	0.999	1.12×10^{1}	-23.26
	KI + MT	1.023	1.000	1.67×10^{2}	-29.99

The parameter values obtained and calculated from the plot are given in Table 4. The calculated ΔG^{o}_{ads} values for all types of halides in the presence and absence of MT were in the range of -20 to -40 kJ mol^{-1}. Generally, it is accepted that the values of ΔG^{o}_{ads} in the order of -20 kJ mol^{-1} or less negative are associated with an electrostatic interaction between the charged inhibitor molecules and

the charged metal surface (physisorption); those of -40 kJ mol^{-1} or more negative involves charge sharing or transfer from the inhibitor molecules to the metal surface to form a co-ordinate covalent bond (chemisorption) [39-40]. From Table 4, it can be observed that in the presence of halide ions alone, the interaction of adsorption are more toward physisorption with ΔG^o_{ads} values range from -11.48 to -26.06 kJ mol^{-1} whereas the values of ΔG^o_{ads} for all combinations of MT with KCl, KBr and KI are between -28.98 to -40.46 kJ mol^{-1} which suggests that the adsorption mechanism of these combinations on the mild steel surface in HCl solution is more towards chemical than physical interaction [41].
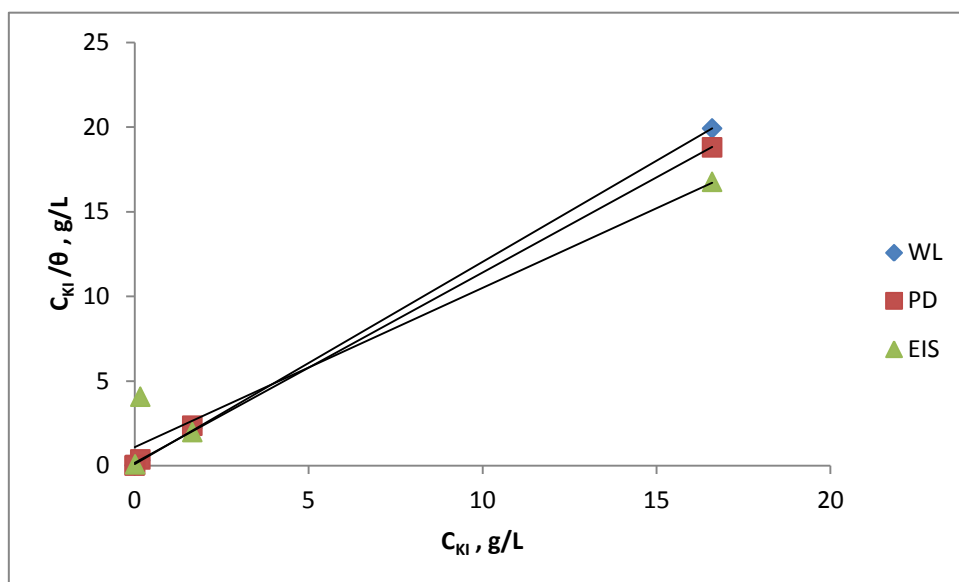
Figure 6. Adsorption isotherms for mild steel in 0.5 M HCl in different concentrations of KI.
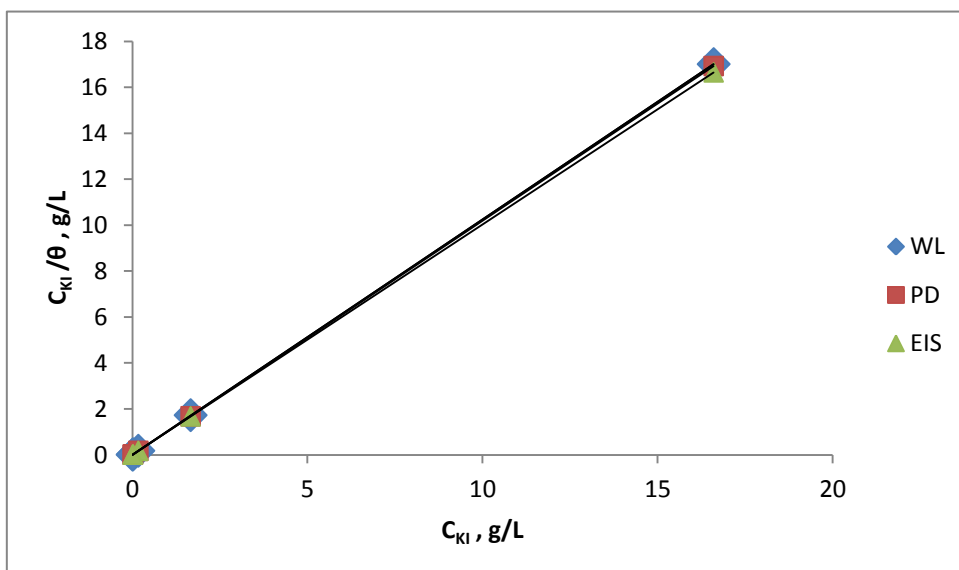
Figure 7. Adsorption isotherms for mild steel in 0.5 M HCl in different concentrations of KI in the presence of MT.

3.5. Synergism of MT with halide ions

All the experimental results have revealed that the addition of halide ions to the inhibited solution enhances the inhibition efficiency and the surface coverage, θ. This behaviour is attributed to the synergistic effect between added halide ions and MT.

To determine the existence of the synergism phenomenon between MT and the halide ions, synergism parameter was evaluated using the equation initially proposed by the Aramaki and Hackermann in 1964 and reported elsewhere [42-44]:

$$S_1 = \frac{1 - I_{1+2}}{1 - I'_{1+2}} \qquad (6)$$

Where $I_{1+2} = I_1 + I_2$; I_1 = inhibition efficiency of the halide ions; I_2 = inhibition efficiency of the MT and I'_{1+2} = measured inhibition efficiency for combination of MT and halide ions.

This parameter was evaluated by the inhibition efficiencies obtained by all techniques. The results obtained are presented in Table 5. The synergistic effect of halide ions with MT is probably due to co-adsorption between these two molecules which may be either competitive or co-operative adsorptions [45]. In competitive adsorption, the anion and cation are adsorbed at different sites on the metal surface while in co-operative adsorption; the anion is chemisorbed on the metal surface and followed by the adsorption of the cation on a layer of anion.

Table 5. Synergism parameters of mild steel in 0.5 M HCl at (27±2 ºC) for different types of halide.

Concentration (+ 3 g L-1 MT)	Weight loss method S1(WL)	Potentiodynamic polarisation method S1(PDP)	EIS method S1(EIS)
1×10^{-5} M KCl	1.37	0.74	0.95
1×10^{-4} M KCl	1.34	0.72	0.96
1×10^{-3} M KCl	1.48	0.73	0.95
1×10^{-2} M KCl	1.67	0.78	0.95
1×10^{-1} M KCl	1.67	0.71	0.94
1×10^{-5} M KBr	1.34	0.64	1.01
1×10^{-4} M KBr	1.32	0.64	1.01
1×10^{-3} M KBr	1.49	0.64	1.02
1×10^{-2} M KBr	1.66	0.72	1.10
1×10^{-1} M KBr	1.71	0.79	1.01
1×10^{-5} M KI	1.34	0.65	1.04
1×10^{-4} M KI	1.26	1.06	1.48
1×10^{-3} M KI	1.45	1.17	1.64
1×10^{-2} M KI	1.66	1.62	1.81
1×10^{-1} M KI	1.73	1.35	1.83

The values of S_1 calculated were mainly more than one which indicates a synergistic effect. In other words, the halide anions will first be chemisorbed onto the mild steel surface and followed by the

adsorption of MT cations on the layer of the halide anions. However, for those values of S_1 less than one especially for potentiodynamic measurements, a co-operative mechanism could have existed between the halide ions and MT cations even though S_1 values indicates antagonistic effect. This can be proven when the addition of the halide ions enhances the inhibition performance of the MT as confirmed earlier by all measurements.

The synergistic effect of the highest concentration of each halide ions (1×10^{-1} M) in all measurements was found to increase in the order Cl < Br < I, which seems to indicate that the radii of halide ions may influence this effect. For example, the iodide ion with a radius of 1.35 Å is more predisposed to adsorption than the bromide ion with a radius of 1.14 Å or the chloride ion with a radius of 0.90 Å. Because of the larger ionic radius, the iodide ion has higher hydrophobicity as compared to the other two halide ions [12]. The adsorption of I^- ions onto the metal surfaces will decrease the hydrophilicity of the metal surfaces, which is likely to promote the adsorption of organic molecule in replace of the water molecules [46]. Thus, the inhibition efficiency of MT is enhanced to a considerable extent in the presence of KI.

4. CONCLUSION

Mangrove tannin was found to inhibit the corrosion of mild steel in 0.5 M HCl solution. The MT and all three halide ions obey the Langmuir adsorption isotherm model. The values of Gibbs free energy of adsorption indicated that MT and halide ions were adsorbed onto the mild steel surface mainly by chemisorption mechanism. The addition of halide ions synergistically improved the inhibition performance of MT due to the co-adsorption effect. The synergism was found to be in the order of KI > KBr > KCl.

References

1. N. Çalışkan and S. Bilgiç, *Appl. Surf. Sci.* 153, (2000) 128
2. A. A. Rahim and J. Kassim, *Recent Pat. Mater. Sci.* 1, (2008) 223
3. P. B. Raja and M. G. Sethuraman, *Mater. Lett.* 62, (2008) 113
4. V. S. Sastri, *Corrosion Inhibitors*, John Wiley & Sons, Ltd. (1998)
5. A. K. Maayta and N. A. F. Al-Rawashdeh, *Corros. Sci.* 46, (2004) 1129
6. M. Elayyachy, A. E. Idrissi and B. Hammouti, *Corros. Sci.* 48, (2006) 2470
7. K. C. Emregül and M. Hayvalí, *Corros. Sci.* 48, (2006) 797
8. L. Wang, *Corros. Sci.* 43, (2001) 2281
9. J. R. Davis, *Corrosion: Understanding the Basic*, ASM International, (2000)
10. A. A. Rahim, E. Rocca, J. Steinmetz, M. J. Kassim, R. Adnan and M. S. Ibrahim, *Corros. Sci.* 49, (2007) 402
11. S. M. A. Shibli and V. S. Saji, *Corros. Sci.* 47, (2005) 2213

12. R. Solmaz, M. E. Mert, G. Kardas, B. Yazici and M. Erbil, *Acta Phys-Chim. Sin.* 24, (2008) 1185
13. F. Bentiss, M. Bouanis, B. Mernari, H. M. Traisnel and M. Lagrenée, *J. Appl. Electrochem.* 32, (2002) 678
14. Y. Harek and L. Larabi, *Kem. Ind.* 53, (2004) 55
15. M. Özcan, R. Solmaz, G. Kardaş and I. Dehri, *Colloids Surfaces A* 325, (2008) 57
16. H. Tavakoli, T. Shahrabi and M. G. Hosseini, *Mater. Chem. Phys.* 109, (2008) 281
17. Y. Feng, K. S. Siow, W. K. Teo and A. K. Hsieh, *Corros. Sci.* 41, (1999) 829
18. I. B. Obot, N. O. Obi-Egbedi and S. A. Umoren, *Corros. Sci.* 51, (2009) 276
19. S. A. Umoren, Y. Li and F. H. Wang, *Corros. Sci.* 52, (2010) 2422
20. S. A. Umoren, O. Ogbobe, I. O. Igwe and E. E. Ebenso, *Corros. Sci.* 50, (2008) 1998
21. M. K. Pavithra, T. V. Venkatesha, K. Vathsala and K. O. Nayana, *Corros. Sci.* 52, (2010) 3811
22. J. Z. Ai, X. P. Guo, J. E. Qu, Z. Y. Chen and J. S. Zheng, *Colloids Surfaces A* 281, (2006) 147
23. X. Li, S. Deng, H. Fu and G. Mu, *Corros. Sci.* 50, (2008) 2635
24. M. Stratmann and G. S. Frankel, *Corrosion and Oxide Films*, Wiley-VCH, (2003)
25. Y. Feng, K. S. Siow, W. K. Teo and A. K. Hsieh, *Corros. Sci.* 41, (1999) 829
26. M. Kissi, M. Bouklah, B. Hammouti and M. Benkaddour, *Appl. Surf. Sci.* 252, (2006) 4190
27. F. S. De Souza and A. Spinelli, *Corros. Sci.* 51, (2009) 642
28. K. F. Khaled, *Appl. Surf. Sci.* 252, (2006) 4120
29. M. Lebrini, M. Lagrene'e, H. Vezin, M. Traisnel and F. Bentiss, *Corros. Sci.* 49, (2007) 2254
30. M. Lagrene'e, B. Mernari, M. Bouanis, M. Traisnel and F. Bentiss, *Corros. Sci.* 44, (2002) 573
31. S. Y. Sayed, M. S. El-Deab, B. E. El-Anadouli and B. G. Ateya, *J. Phys. Chem. B* 107, (2003) 5575
32. M. Behpour, S. M. Ghoreishi, N. Soltani and M. Salavati-Niasari, *Corros. Sci.* 51, (2009) 1073
33. K. F. Khaled, *Corrosion Science* 52, (2010) 3225
34. W. A. W. Elyn Amira, A. A. Rahim, H. Osman. K. Awang and P. Bothi Raja, *Int. J. Electrochem. Sci.* 6, (2011) 2998
35. A. Popova, E. Sokolova, S. Raicheva and M. Christov, *Corros. Sci.* 45, (2003) 33
36. S. A. Umoren, Y. Li and F. H. Wang, *Corros. Sci.* 52, (2010) 1777
37. A. M. Abdel-Gaber, B. A. Abd-El-Nabey and M. Saadawy, *Corros. Sci.* 51, (2009) 1038
38. A.Y. Musa, A. A. H. Kadhum, A. B. Mohamad, A. A. B. Rahoma and H. Mesmari, *J. Mol. Struct.* 969, (2010) 233
39. X. Li, S. Deng and H. Fu, *Corros. Sci.* 52, (2010) 3413
40. O. K. Abiola and N. C. Oforka, *Mater. Chem. Phys.* 83, (2004) 315
41. R. Solmaz, E. Altunbas and G. Kardas, *Mater. Chem. Phys.* 125, (2011) 796
42. G. K. Gomma, *Mater. Chem. Phys.* 54, (1998) 241
43. E. E. Oguzie, B. N. Okolue, E. E. Ebenso, G. N. Onuoha and A. I. Onuchukwu, *Mater. Chem. Phys.* 87, (2004) 394
44. E. E. Ebenso, *Mater. Chem. Phys.* 79, (2003) 58
45. G. Schmitt and K. Bedbur, *Werks. Korros.* 36, (1985) 273
46. Y.I. Kuznetsov and N.N. Andreev, *Corrosion 96, NACE International, Houston,* paper No. 214.